Bilateral Symmetry in Central Retinal Blood Vessels*

Sangeeta Biswas**
Centre of Excellence IT4Innovations
Faculty of Information Technology
Brno University of Technology
Brno 61200, Czech Republic
biswas@fit.vutbr.cz

Johan Rohdin
Centre of Excellence IT4Innovations
Faculty of Information Technology
Brno University of Technology
Brno 61200, Czech Republic
rohdin@fit.vutbr.cz

Martin Drahansky
Centre of Excellence IT4Innovations
Faculty of Information Technology
Brno University of Technology
Brno 61200, Czech Republic
drahan@fit.vutbr.cz

***Abstract*—Symmetry can be defined as uniformity, equivalence or exact similarity of two parts divided along an axis. While our left and right eyes clearly have a high degree of external bilateral symmetry, it is less obvious to what degree they have internal bilateral symmetry. This is especially true for central retinal blood vessels (CRBVs) which are responsible for supplying blood to retinas and also can be used as a strong biometric. In this paper, we study whether CRBVs of the left and right retinas possess strong enough bilateral symmetry so that we reliably tell whether a pair of CRBVs of the left and right retinas belongs to a single person. We evaluate and analyse the performance of both human and neural network based bilateral CRBVs verification. By experimenting on a large publicly available data set, we confirm that CRBVs have bilateral symmetry to some extent.**

***Index Terms*—retina, symmetry, central retinal blood vessels, deep neural network**

I. Introduction

Symmetry can be defined as *uniformity*, *equivalence* or *exact similarity* of two parts divided along an axis. Paired organs such as eyes, ears, hands, legs, etc., give an approximate-bilateral symmetrical look (i.e. almost identical left and right forms) to the exterior of our human body by dividing it into two parts through an imaginary left-right axis. Symmetrical left and right eyes not only give us a sense of beauty but also full field of vision and depth of perception. Even though we can easily see outward symmetry in our left and right eyes, seeing symmetry in the internal parts of our two eyes is not easy. This is especially true for the retina which is a thin, semi-transparent, multi-layered, neural tissue that covers two-thirds of the interior of our each eye. It is anatomically and physiologically considered as an extension of our brain. It is mainly responsible for converting incoming electromagnetic signals from the world outside of our eye into neural signals, and then handing the neural signals to the optic nerves. The neural signals, relaying through the optic nerves, form images into the visual cortex of our brain, and therefore, we can have a sense of vision [1], [2]. Any kind of disturbance in retina can have negative effect on our vision. Severe pathology in retina even can cause irreversible partial or complete vision loss.

The retina is one of the most metabolically active tissues in the human body. It consumes high level of oxygen and nutrients to ensure our visual functionality. Two kinds of well-organized blood vessels, central retinal blood vessels (CRBVs) and choroidal blood vessels (CBVs), are responsible for supplying oxygen and nutrients to the retina, as well as transporting away waste from the retina. Not only for their contribution in our visual system, but also for their unique and almost lifetime permanent patterns, CRBVs and CBVs draw huge research interest [3]–[21]. They are considered as retina based biometric, and used for identifying individuals in order to control the access to highly confidential and secured environments.

In medical science, bilateral symmetry between different anatomical structures and layers of the left and right retinas is a well studied topic under the term *interocular symmetry* [22]–[27]. It helps ophthalmologists to use one retina as a proxy of the other retina as well as to detect development of pathology in the retina. In retina based biometric, bilateral symmetry may open a possibility of developing side independent retina based person authentication system in which one side retina can be used to access a system developed for the opposite side retina. This will increase user flexibility especially when the registered retina is affected by severe pathology. The study of bilateral symmetry may also help us to understand how strong a biometric system would be if both side retinas are used. If the left and right retina of a person were completely different then an authentication system using both side retina would be *two times stronger* than an authentication system using one side retina. However, with the exception of our previous works (i.e., [28], [29]), studies on bilateral symmetry are almost non-existent in the retina based biometric research. In [28], [29], we reported that in color fundus photographs as well as in CRBVs segmented from the color fundus photographs, it is possible to see similarity between two retinas, and, therefore, to decide whether a pair of a left and a right retinal images belongs to the same person or to two different persons.

*This work was supported by The Ministry of Education, Youth and Sports of the Czech Republic from the National Programme of Sustainability (NPU II); project IT4Innovations excellence in science - LQ1602.

**The author is also affiliated with the Faculty of Engineering, University of Rajshahi, Rajshahi 6205, Bangladesh.

978-1-7281-6232-4/20/$31.00 ©2020 IEEE

In this paper, we try to find bilateral symmetry in CRBVs. Our work in this paper is similar to our previous works [28], [29]. Differences are that our previous works were based on the opinion of only four untrained volunteers and on very small data sets. Moreover, the simple similarity measurements (i.e., structural similarity and cosine similarity) used in our previous works were highly prone to the orientation of the optic disc and macula. Therefore, we could not claim anything firmly based on our findings. In this paper, we report the results of 20 untrained volunteers. The volunteers are asked to find the similarity between pairs of CRBVs without being instructed what to look for or where to look. Instead of simple similarity measurements, we train a Y shaped neural network (YNN) to find bilateral symmetry. We do experiments on a set of $1,752$ pairs of CRBVs, which is much larger than the largest set used in our previous works, which had only 64 pairs.

II. Background

A. Brief Description of CRBVs

The approximately 0.5 mm thick retina is sandwiched between the avascular vitreous and the highly vascular choroid. Branching out from the ophthalmic blood vessels, CRBVs pierce the optic nerve and enter the internal side of the retina through the optic disc (as shown in Fig. 1(a)). On the other hand, branching out from the ophthalmic blood vessels, cilliary blood vessels enter the choroid and form CBVs to supply blood to-and-from the external side of the retina by diffusion. The internal side of the retina is the side that comes first when we look at a retina from the outside through the lens and the vitreous. It is composed of eight basic layers: internal limiting membrane (ILM), retinal nerve fiber layer (RNFL), ganglion cell layer (GCL), inner plexiform layer (IPL), inner nuclear layer (INL), outer plexiform layer (OPL), outer nuclear layer (ONL) and outer limiting membrane (OLM). On the other hand, the external side is the side of the retina which is close to the choroid. It is composed of the photoreceptor layer (PRL) and the retinal pigment epithelium (RPE) layer [1], [2]. Using the optical coherence tomography (OCT), we can see these layers as well as CRBVs (see Fig. 1(b)).

Even though it is possible to see blood vessels in deeper layers of retina in OCT photographs, until now retina biometric research is mainly based on fundus photographs. As shown in Fig. 1(c), in a color fundus photograph, we can see the almost circular, colored foreground of a retina on a dark background. Most of the foreground of a retina is covered by tree structured central retinal arteries (CRAs) and central retinal veins (CRVs). The CRAs and CRVs together form the CRBVs. Other anatomical structures such as macula, fovea, optic disc (OD), optic cup (OC), neuroretinal rim (NR), are also visible in a color fundus photograph. Depending on the fundus camera, we may see a side indicator (i.e., triangle or oval shaped bump) always at the right side which helps us determine whether it is a left or right side retina. If OD is in the same side as the side indicator (SI) in a retinal image, then that image belongs to a right-side retina. If OD is in the opposite side of SI, then that image belongs to a left side retina.

Coming out from the OD on the nasal side, the CRBVs form four branches: inferior, superior, nasal and temporal branches. The first bifurcation of the CRBVs can be occurred inside the optic nerve, or at the mouth of OD, or a bit upper of the OD. There is no CRBV in the center of the fovea, i.e., in the foveal avascular zone (FAZ). The CRAs appear, in general, bright red when compared to the purple-red CRVs. Generally, the CRAs have smaller caliber than the CRVs inside the OD area as well as surrounding the OD area. Near to the boundary of the foreground of the retina, it is hard to distinguish CRVs from CRAs either by color or by caliber, though.

B. CRBVs as Biometric

Last 120 years the CRBVs have been playing an important role in retina based biometric which is considered to be one of the high performing biometrics. In 1899, Dr. Levinsohn first mentioned in one of his German articles that retinal images can be used for human identification. Along with the size and shape of the OD, and its border, he mainly considered the arrangement of the CRBVs to distinguish humans from each other. In 1918, Haber showed that by placing a fine screen in front of the fundus photographic plate, CRBVs can be represented as a sketch on a chess board. Later Dr. Blascheck wrote a formula in his unpublished work to distinguish individuals considering the external appearances of the OD and macula, visibility of the CBVs, atrophy of the choroid, certain permanent abnormalities such as as coloboma, etc., the location of the first bifurcation of the CRA, and the number of the CRVs and the CRAs intersecting two parallel lines in the superior and inferior parts and the crossing patterns of the CRAs and CRVs through those lines from the left to the right. Details of these works can be found in Türkel's book [30] written in German and a short note in English can be found in [4]. In 1935, Dr. Simon and Dr. Goldstein claimed in [3] that even though the patterns of both CRAs and CRVs can be jointly used for human classification, only CRVs are good enough, since they have more distinctive appearance than the CRAs, being larger and their lumen photographing darker.

In the patent US 4,109,237 [6], the patterns of CRBVs of subjects were captured by illuminating the retina by visible monochromatic green light, since this light is absorbed by the dark red of blood vessels and substantially reflected by the retinal tissue which results a high contrast between tissue and vessels. Later it was found that the brightness of the visible illuminating light needed in order to get a recognizable pattern, caused discomfort to the subjects being identified. It also caused the pupil of the eye to constrict, making it more difficult to get CRBVs pattern. Therefore, in the later patents such as US 4,393,366 [7], US 4,620,318 [8], US 5,532,771 [10], etc., near infrared (IR) light was used. The wavelength of IR light is invisible to human eye, therefore, subjects do not feel any discomfort. Moreover, it has a cost saving advantage as well. However, scanning with IR light provides reflections from the CRBVs as well as the CBVs. In fact, CBVs reflect most of the

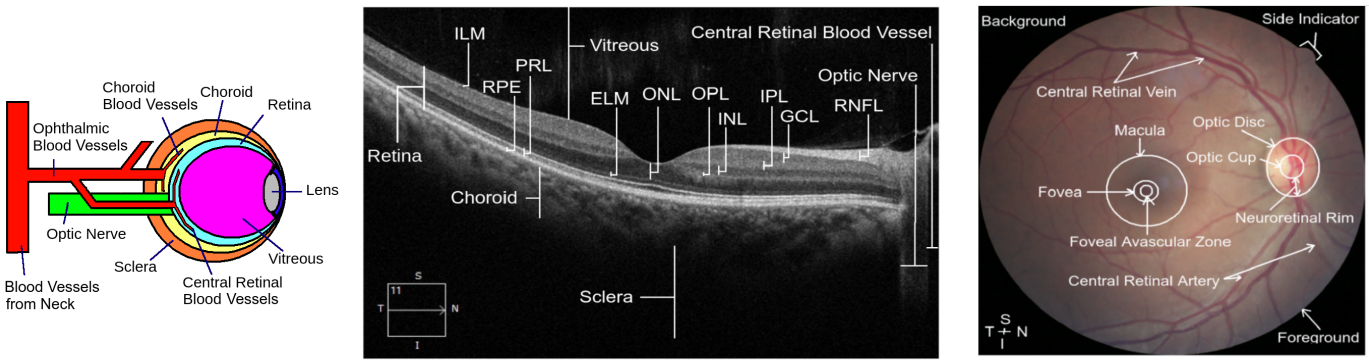

(a) (b) (c)

Fig. 1. (a) Very simple schematic diagram of human eye drawn to understand the blood supply to-and-from the retina. (b) Visibility of different layers of a healthy right side retina in a OCT photograph. S: Superior, I: Inferior, N: Nasal and T: Temporal. (c) Visibility of main anatomical structures in a color fundus photograph of a healthy right retina. Note that, the boundaries of macula, fovea, FAZ, OD, OC, NR are not accurately drawn.

useful information needed to identify subjects. Therefore, in IR based retina identification system, the contribution of CRBVs is very small. Since choroid is not a part of retina but is located underneath the retina, it is a bit misleading to consider CBVs as a retina based biometric. However, *retina identification* is a familiar term, therefore, CBVs based identification is also termed as retinal identification [9].

Research works [12]–[19], [21] considered only the features extracted from the CRBVs, such as ridge endings, ridge bifurcations, crossovers, vessels' diameter size, vessels' position and orientation, skeleton of the whole structure of CRBVs, and so on, for authentication.

III. Our Approach

None of our paired body organs have identical left and right forms. That means our human body show *approximate-bilateral* or *pseudo-bilateral* symmetry instead of *perfect-bilateral* symmetry. And this approximate-bilateral symmetry is generally less obvious inward than outward for paired organs. It is in particular true for our eyes, especially when 2D color fundus photographs are used for left and right retinas. The unique tree like structure of the CRBVs spreading over the retina gives an interretinal asymmetrical look to color fundus photographs at the first glance. Poor quality of retinal image can increase this asymmetrical look by displaying different colors as well as overexposing and under exposing different parts of the CRBVs. Many factors such as experience level of the operator, operator's finger movement or shaking, different settings of fundus cameras, subject's eye movement or blinking, different amounts of light reflection by different parts of retina because of its natural curved structure, inadequate illumination, variation of pupil dilation, poor focus, lossy compression-decompression techniques, noisy transmission channels and so on can result in poor quality retinal images. Beside these factors, some pathology can have unilateral effects which can cause asymmetry. Therefore, in order to check bilateral symmetry in CRBVs, we do not expect to see a perfect mirror or reflection symmetry, especially when we work on publicly available data.

Instead of measuring length or caliber of CRBVs, as is typical in research of medical science, we investigate if it is possible to tell whether a pair of the CRBVs of the left and right retinas belong to a single person or to two different persons. Our assumption is that when there is substantial bilateral symmetry in such a pair, there is a high probability that the pair belongs to a single person. In order to support our assumption we took opinions from 20 volunteers along with one deep neural network based system. In order to get rid of the effect of color or different anatomical structures of retina (i.e., OD, macula, etc.,), we segmented CRBVs using a U shaped convolutional neural network (U-Net) [31].

A. Experimental Setup

We did all implementations using TensorFlow's Keras API 2.1.6-tf and Python. We used a standard PC with Intel(R) Core(TM) i9-9900K having 8 Cores and 31 GB memory, and with two NVIDIA GeForce GTX 1080 GPUs having 8 GB Memory per GPU.

To segment CRBVs from RGB colored retinal images, we trained a U-Net which is well-known for its requirement of very few images in the training phase. For example, in [31], only 30 images were used to train a U-Net which outperformed a sliding window CNN for the ISBI neuronal structures in EM stacks challenge 2012. We used 40 RGB images, and their corresponding manually segmented CRBVs of a publicly available data set named DRIVE [32] to train our U-Net. As a validation set we used 28 RGB retinal images and their corresponding manually segmented CRBVs of another publicly available data set named CHASE_DB1 [33]. Figure 2 shows the model architecture of our U-Net. We set *mean-squared-error (mse)* as the loss function; RMSProp with a learning rate of 0.001 as the optimizer and $mini\_batch\_size = 8$. After 3400 iterations, we achieved 0.021 mse.

To do the verification, we used RGB retinal images of the Kaggle data set [34], provided by EyePACS, and publicly available via Kaggle online community of data scientists and machine learners for the competition of diabetic retinopathy detection. This database has $42,111$ pairs of images. In each

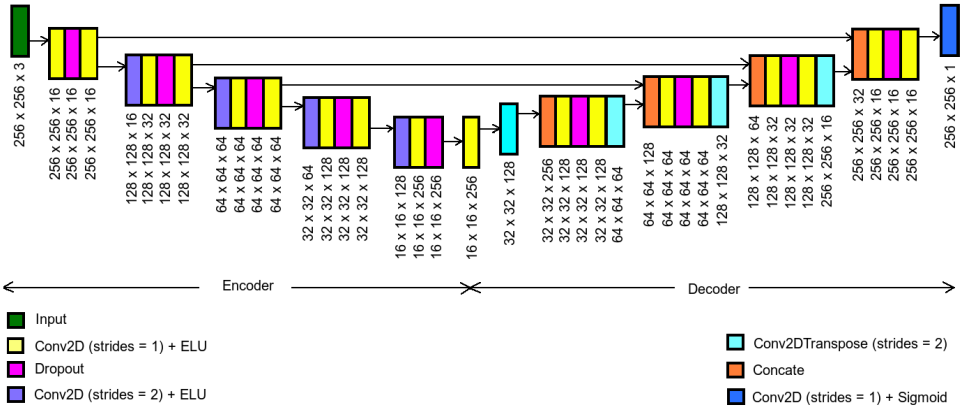

Fig. 2. Architecture of U-Net used to extract CRBVs from RGB retinal images.

pair there is a left and a right retinal image belonging to a single subject ID. Therefore, there is in total $84,222$ RGB retinal images belonging to $42,111$ subject IDs. There are 27 types of resolutions. We chose images with resolutions 3264×4928 and 3168×4752, because the foreground of these two resolutions have complete circular shape.

We prepared three sets i.e., Kaggle_A, Kaggle_B and Kaggle_C, from our chosen images for three purposes (see Table I for details). We prepared two test sets (i.e., Kaggle_SetA.1 and Kaggle_SetA.2) using the images of Kaggle_SetA, and one test set (i.e., Kaggle_SetC) using the images of Kaggle_SetC. In principle, it is possible to build 150 positive pairs (i.e., the left and right retinal images of a pair belonging to a single subject ID) and $150 \times 149 = 22,350$ negative pairs (i.e., the left and right retinal images of a pair belonging to two different subject IDs) using the 150 pairs of Kaggle_SetA. However, for human volunteers it is difficult and time consuming to give decision about $150 + 22,350 = 22,500$ pairs. Therefore, we decided to reduce the number of pairs while keeping the variability among pairs as much as possible. For fulfilling that, we divided 150 subjects into 3 groups: the first 50 subjects were for the positive pairs (PPs), the second 50 were for the left side of negative pairs (NPs) and the third 50 were for the right side of NPs. In this way, we kept only 50 PPs and $50 \times 50 = 2,500$ NPs in Kaggle_SetA.1, and 50 PPs and 50 NPs in Kaggle_SetA.2. The PPs were the same in both test sets, whereas the NPs of Kaggle_SetA.2 were a subset of the NPs of Kaggle_SetA.1. In Kaggle_SetC, there were $1,752$ PPs and $1,752$ NPs. Even though it was possible to make $1,752 \times 1,751 = 3,067,752$ NPs from $1,752$ pairs, we chose only $1,752$ NPs in order to keep a balance between the PPs and NPs. Contrary to Kaggle_SetA.1 and Kaggle_SetA.2, there was subject overlap between the PPs and NPs, as well as between the left and right sets of NPs in Kaggle_SetC.

Since the background dark pixels do not provide any necessary information, the background was cropped so that the foreground could touch the boundary without loosing any important pixels of the foreground. Because of different resolutions of different data sets, we re-sized all images to 256×256 by bicubic interpolation. Then we re-scaled pixel values to $[0, 1]$ for simple contrast stretching. Except that, no other pre-processing was applied to any images.

TABLE I
DATA SETS USED FOR VERIFICATION.

Data Set	Resolution	# Pairs	Purpose
Kaggle_SetA	3264×4928	150	manual and automatic verification
Kaggle_SetB	3168×4752	7034	training YNN
Kaggle_SetC	3264×4928	1752	only automatic verification

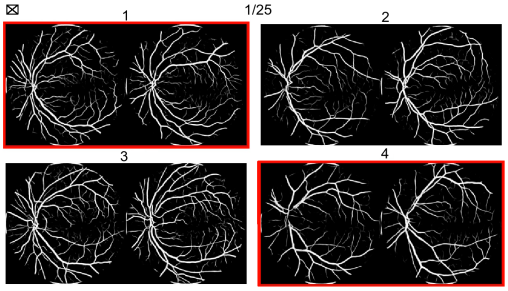

Fig. 3. An example frame for collecting volunteers' opinions. When a volunteer clicked on any pair its boundary turned into red color and it meant that the volunteer considered that pair belonged to a single person. Numbers 1, 2, 3, 4 were the pair numbers, $19/25$ was the frame number and *cross* sign was for closing the frame.

B. Manual Verification

For manual verification, we asked 20 untrained volunteers who did not know where to find symmetrical properties in retinas to participate in a test. In this test, 25 frames were shown to each volunteer, where each frame contained four pairs of CRBVs side-by-side (as shown in Fig. 3). The right side CRBVs were flipped to make the comparison task easier for the human volunteers. All volunteers (i.e., ID 1-20) saw the same 50 PPs but in random orders. Different volunteers with ID 1-10 saw 50 different NPs which were randomly chosen from the $2,500$ NPs of Kaggle_SetA.1, so that they were not exhausted by seeing too many NPs. Volunteers with ID 11-20 saw the same 50 NPs but in random orders.

The task of the human volunteers was to click on a pair when they thought there is high probability that pair belongs to a single person. Volunteers were allowed to select/deselect any pair as many times as they wanted and spent as much time on the verification task as they wanted. But after closing any frame they were not allowed to see the previous frame any more. After closing the last frame, each volunteers were asked to write about what factors they considered in order to make a decision. Twenty volunteers participated in 20 separate sessions. None of them were aware about the true answers. All volunteers were requested not to share their assumptions with other volunteers. When writing their points, they were informed of retina related terms to make their writing easier.

As shown in Fig. 4, there were some easily recognizable positive pairs (see the 1^{st} and 3^{rd} row of Fig. 4) in Kaggle_SetA.1 and Kaggle_SetA.2, which were recognized by all volunteers and some difficult pairs which confused almost all volunteers (see the 2^{nd} and 4^{th} row of Fig. 4). Even though most of the volunteers were not familiar with CRBVs segmented from color fundus photographs, they were able to see strong similarity in some PPs and strong dissimilarity in some NPs by considering different factors. Many volunteers considered segmented CRBVs as venation i.e., the arrangement of veins in a leaf. Some of the factors figured out by the untrained volunteers are thickness of clearly visible CRBVs; overall structure of CRBVs looking from the far; angles of CRBVs while leaving the root (i.e., OD area), branching pattern; grouping tendency of vessels; vessel pattern close to the empty space (i.e., macula); curvature of the thickest/thicker vessel(s) considering straightness and tortuosity (or waviness) of vessel(s); density of vessels; alignment of the root (i.e., OD) with the empty space (i.e., macula); how vessels are spreading, and so on. Some factors overlapped within some volunteers. As shown in Table II, even the lowest performance was more than a random chance.

Our summary is that it is not easy to see bilateral symmetry in grayscaled pairs of segmented CRBVs. It is hard to figure out similarity/dissimilarity between a pair of CRBVs especially when we do not have pre-knowledge. This task becomes harder when the images do not have the same alignment of OD and macula, because different alignment can make even two images of CRBVs taken from the same retina look different. Even the quality of the color fundus photographs and the existence of pathology also play important roles. The U-Net may end up segmenting very few or discontinuous CRBVs from poor quality fundus photographs. Some pathology (such as retinal hemorrhages) can cause some parts of the blood vessels to be invisible, which can make a pair of CRBVs from the same person look different.

C. Automatic Verification

We trained a deep neural network having a lying Y shaped architecture (YNN) as shown in Fig 5. We set *binary crossentropy* as the loss function; RMSProp with a learning rate of 0.0001 as the optimizer. For all other settings, we used the default values of TensorFlow's Keras API 2.6.1-tf. Contrary

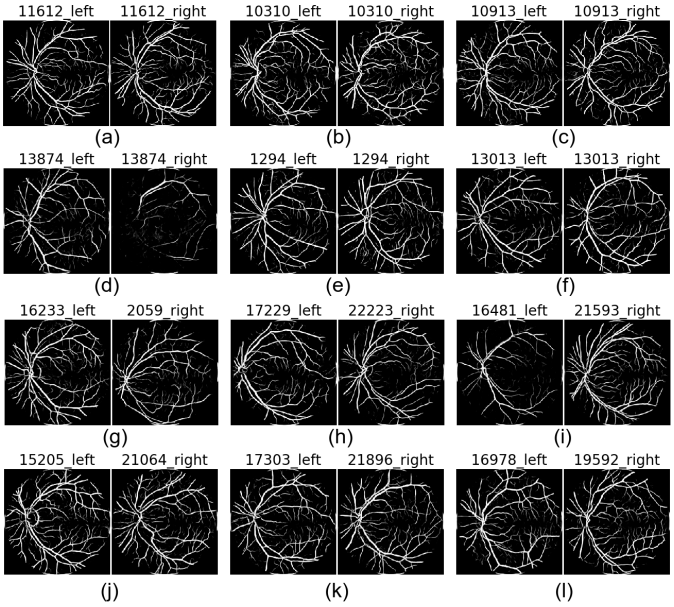

Fig. 4. 1st row: three easily recognized PPs in Kaggle_SetA.1 and Kaggle_SetA.2 [(a) & (b)] two PPs recognized by all 20 volunteers, and (c) a PP recognized by 19 out of 20 volunteers. 2nd row: three difficult PPs. (d) a PP recognized by only 1 out of 20 volunteers, [(e) & (f)] two PPs recognized by 6 out of 20 volunteers. 3rd Row: three easily recognized NPs in SetA.2. [(g), (h) & (i)] three NPs decided by 10 out of 10 volunteers. 4th Row: three difficult NPs. [(j), (k) & (l)] three NPs selected as PPs by 9, 8 and 7 out of 10 volunteers, respectively.

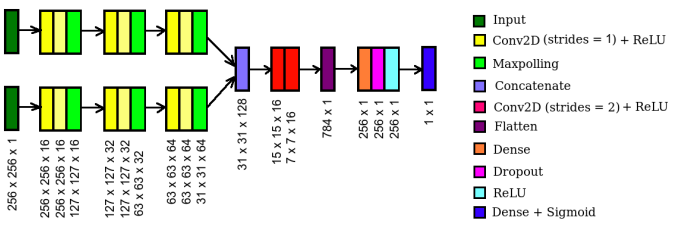

Fig. 5. Architecture of automatic verifier. Vertical text shows the output shape of the corresponding layer.

to standard verification tasks, e.g., hand written signature, face and voice, the left and right retina are, although approximately symmetric, not the same entity so it is not obvious that they should be processed in the same way. Therefore, we tried both tied and untied weights for the two legs of YNN. The output of the concatenate layer of YNN showed that it looked thick blood vessels, area surrounding OD and macula, and so on, to make its features. As shown in Table II, the tied YNN was marginally better than the untied YNN, and both YNNs performed clearly better than the human volunteers. However, it is important to notice that, contrary to the human volunteers, the automatic system made use of labeled training data. Volunteers would have better performance if they could get opportunity to train themselves before participating the manual verification task.

TABLE II
RESULTS OF MANUAL AND AUTOMATIC VERIFICATION. [AVG.: AVERAGE]

	Kaggle_SetA.1											Kaggle_SetA.2												Kaggle_SetC	
	Untrained Volunteers											Untrained Volunteers											YNN		YNN	
Volunteer ID	1	2	3	4	5	6	7	8	9	10	Avg.	11	12	13	14	15	16	17	18	19	20	Avg.	Untied	Tied	Untied	Tied
Accuracy (%)	64	66	66	71	77	74	62	66	72	65	68.3	66	68	69	76	69	72	76	66	63	69	69.4	88	89	85	88
Precision (%)	62	62	90	72	75	87	57	71	89	63	72.8	72	70	73	73	69	76	77	72	81	68	73.1	81	83	77	80
Recall (%)	74	82	36	68	80	56	92	54	50	70	66.2	52	64	60	82	70	64	74	52	34	72	62.4	100	98	99	99
F1 Score (%)	67	71	51	70	78	68	71	61	64	67	66.8	60	67	66	77	69	70	76	60	48	70	66.3	89	90	87	89

IV. CONCLUSION

Is there any similarity between the central retinal blood vessels (CRBVs) of the left and right retinas of human eyes? Our answer is *yes, there is*. Based on previous works by other researchers, our own analysis and investigation, findings of 20 volunteers and a deep neural network, we can say that CRBVs in our two eyes possess enough similarity so that we can decide whether a pair of left and right retina belong to a single person or to two different persons. However, there is space for a debate on whether that much similarity is good enough for using the term, *bilateral symmetry*. We hope our findings would help us to develop side independent central retinal blood vessels based biometric systems in future which would give more flexibility to users especially when user's registered retina is highly affected by severe pathology.

REFERENCES

[1] S. C. Nemeth, C. Shea, M. DiSclafani, and M. Schluter, *The Posterior Segment*, chapter 9, pp. 88–99, Slack Incorporated, Thorofare, NJ, USA, 2 edition, 2008.

[2] M. D. Abràmoff, M. K. Garvin, and M. Sonka, "Retinal imaging and image analysis," *IEEE Reviews in Biomedical Engineering*, vol. 3, pp. 169–208, 2010.

[3] C. Simon and I. Golstein, "A New Scientific Method of Identification," *New York State Journal of Medicine*, vol. 35, no. 18, pp. 901–906, 1935.

[4] M. E. O'Neill, "A "New" Method of Identification," *Journal of Criminal Law and Criminology*, vol. 26, no. 4, pp. 608–610, 1935.

[5] P. Tower, "The Fundus Oculi in Monozygotic Twins: Report of Six Pairs of Identical Twins," *Archives of Ophthalmology*, vol. 54, pp. 225–239, 1955.

[6] R. B. Hill, "US4109237: Apparatus and Method for Identifying Individuals Through Their Retinal Vasculature Patterns," 1978.

[7] R. B. Hill, "US 4,393,366: Rotating Beam Ocular Identification Apparatus and Method," 1983.

[8] R. B. Hill, "US 4,620,318: Fovea-Centered Eye Fundus Scanner," 1986.

[9] R. B. Hill, *Retina Identification*, pp. 123–141, Springer US, 1996.

[10] J. C. Johnson and R. B. Hill, "US 5,532,771: Eye Fundus Optical Scanner System and Method," 1996.

[11] J. Marshall and D. Usher, "US 6,453,057: Method for Generating a Unique Consistent Signal Pattern for Identification of an Individual," 2002.

[12] Z.-W. Xu, X.-X. Guo, X.-Y. Hu, and X. Cheng, "The blood vessel recognition of ocular fundus," in *ICMLC*, 2005, vol. 7, pp. 4493–4498.

[13] C. Mariño, M. G. Penedo, M. Penas, M. J. Carreira, and F. Gonzalez, "Personal authentication using digital retinal images," *Springer PAA*, vol. 9, no. 1, pp. 21–33, 2006.

[14] H. Farzin, H. Abrishami-Moghaddam, and M. Moin, "A Novel Retinal Identification System," *EURASIP JASP*, vol. 2008, pp. 280635, 2008.

[15] A. Arakala, J. S. Culpepper, J. Jeffers, A. Turpin, S. Boztaş, K. J. Horadam, and A. M. McKendrick, "Entropy of the Retina Template," in *Advances in Biometrics*, M. Tistarelli and M. S. Nixon, Eds. 2009, pp. 1250–1259, Springer Berlin Heidelberg.

[16] M. Ortega, M. G. Penedo, J. Rouco, N. Barreira, and M. J. Carreira, "Personal verification based on extraction and characterisation of retinal feature points," *Elsevier JVLC*, vol. 20, pp. 80–90, 2009.

[17] Mikael Agopov, "Retinal identification," in *Biometrics*, Jucheng Yang, Ed., chapter 5. IntechOpen, Rijeka, 2011.

[18] W. Barkhoda, F. Akhlaqian, M. D. Amiri, and M. S. Nouroozzadeh, "Retina identification based on the pattern of blood vessels using fuzzy logic," *EURASIP JASP*, vol. 113, 2011.

[19] S. M. Lajevardi, A. Arakala, S. A. Davis, and K. J. Horadam, "Retina Verification System Based on Biometric Graph Matching," *IEEE TIP*, vol. 22, no. 9, pp. 3625–3635, 2013.

[20] F. Sadikoglu and S. Uzelaltinbulat, "Biometric Retina Identification Based on Neural Network," in *Procedia Computer Science*, 2016, vol. 102, pp. 26–33.

[21] M. Frucci, D. Riccio, G. S. di Baja, and L. Serinoa, "Using direction and score information for retina based person verification," *Expert Systems with Applications*, vol. 94, pp. 1–10, 2017.

[22] D. L. Budnez, "Symmetry Between the Right and Left Eyes of the Normal Retinal Nerve Fiber Layer Measured with Optical Coherence Tomography (An Aos Thesis)," *Elsevier AJO*, vol. 106, pp. 252–275, 2008.

[23] H. Li, P. R. Healey, Y. M. Tariq, E. Teber, and P. Mitchell, "Symmetry of Optic Nerve Head Parameters Measured by the Heidelberg Retina Tomograph 3 in Healthy Eyes: The Blue Mountains Eye Study," *Elsevier AJO*, vol. 155, no. 3, pp. 518–523, 2013.

[24] M. Yang, W. Wang, Q. Xu, S. Tan, and S. Wei, "Interocular symmetry of the peripapillary choroidal thickness and retinal nerve fibre layer thickness in healthy adults with isometropia," *BMC Opthalmology*, vol. 16, pp. 182, 2016.

[25] M. Zhou, B. Lu, J. Zhao, Q. Wang, P. Zhang, and X. Sun, "Interocular Symmetry of Macular Ganglion Cell Complex Thickness in Young Chinese Subjects," *PLoS ONE*, vol. 11, no. 7, 2016.

[26] G. Liu, K. Keyal, and F. Wang, "Interocular Symmetry of Vascular Density and Association with Central Macular Thickness of Healthy Adults by Optical Coherence Tomography Angiography," *Scientific Reports*, vol. 7, no. 1, pp. 16297, 2017.

[27] R. Mastey, M. Gaffney, K. Litts, C. Langlo, E. Patterson, M. Strampe, A. Kalitzeos, M. Michaelides, and J. Carroll, "Assessing the Interocular Symmetry of Foveal Outer Nuclear Layer Thickness in Achromatopsia," *TVST*, vol. 8, pp. 21, 10 2019.

[28] S. Biswas, J. Rohdin, T. Mňuk, and M. Drahanský, "Is there any similarity between a person's left and right retina?," in *BIOSIG*, 2019, pp. 1–8.

[29] S. Biswas, J. Rohdin, and M. Drahansky, "Suitable Embedding to Find Similarity Between Left and Right Retinas of a Person," in *CISP-BMEI*, 2019, pp. 1–6.

[30] S. Türkel, *Das Auge als Identifizierungsgrundlage: unter Berücks. von Blascheks Photofundoskopie*, chapter III, pp. 22–41, Slack Incorporated, Graz, 1927.

[31] O. Ronneberger, P. Fischer, and T. Brox, "U-net: Convolutional Networks for Biomedical Image Segmentation," *MICCAI*, vol. 9351, pp. 234–241, 2015.

[32] J. J. Staal, M. D. Abramoff, M. Niemeijer, M. A. Viergever, and B. van Ginneken, "Ridge based vessel segmentation in color images of the retina," *IEEE TMI*, vol. 23, no. 4, pp. 501–509, 2004.

[33] C. G. Owen, A. R. Rudnicka, R. Mullen, S. A. Barman, D. Monekosso, P. H. Whincup, J. Ng, and C. Paterson, "Measuring retinal vessel tortuosity in 10-year-old children: Validation of the computer-assisted image analysis of the retina (caiar) program," *IOVS*, vol. 50, pp. 2004–2010, 2009.

[34] J. Cuadros and G. Bresnick, "EyePACS: An Adaptable Telemedicine System for Diabetic Retinopathy Screening," *SAGE JDST*, vol. 3, no. 3, pp. 509–516, 2009.